J Mater Sci: Mater Med (2012) 23:2563–2573
DOI 10.1007/s10856-012-4716-1

# In vitro cytotoxicity of surface modified bismuth nanoparticles

**Yang Luo · Chaoming Wang · Yong Qiao · Mainul Hossain · Liyuan Ma · Ming Su**

Received: 9 April 2012 / Accepted: 26 June 2012 / Published online: 17 July 2012


**Abstract** This paper describes in vitro cytotoxicity of bismuth nanoparticles revealed by three complementary assays (MTT, G6PD, and calcein AM/EthD-1). The results show that bismuth nanoparticles are more toxic than most previously reported bismuth compounds. Concentration dependent cytotoxicities have been observed for bismuth nanoparticles and surface modified bismuth nanoparticles. The bismuth nanoparticles are non-toxic at concentration of 0.5 nM. Nanoparticles at high concentration (50 nM) kill 45, 52, 41, 34 % HeLa cells for bare nanoparticles, amine terminated bismuth nanoparticles, silica coated bismuth nanoparticles, and polyethylene glycol (PEG) modified bismuth nanoparticles, respectively; which indicates cytotoxicity in terms of cell viability is in the descending order of amine terminated bismuth nanoparticles, bare bismuth nanoparticles, silica coated bismuth nanoparticles, and PEG modified bismuth nanoparticles. HeLa cells are more susceptible to toxicity from bismuth nanoparticles than MG-63 cells. The simultaneous use of three toxicity assays provides information on how nanoparticles interact with cells. Silica coated bismuth nanoparticles can damage cellular membrane yet keep mitochondria less influenced; while amine terminated bismuth nanoparticles can affect the metabolic functions of cells. The findings have important implications for caution of nanoparticle exposure and evaluating toxicity of bismuth nanoparticles.

Y. Luo · C. Wang · Y. Qiao · M. Hossain · L. Ma · M. Su (✉)
NanoScience Technology Center, University of Central Florida, Orlando, FL 32826, USA
e-mail: mingsu@mail.ucf.edu

Y. Luo
Department of Laboratory Medicine, Southwest Hospital, Third Military Medical University, Chongqing 400038, China

C. Wang · M. Su
Department of Mechanical, Materials and Aerospace Engineering, University of Central Florida, Orlando, FL 32826, USA

M. Hossain
School of Electrical Engineering and Computer Science, University of Central Florida, Orlando, FL 32826, USA

**Abbreviations**

| | |
|---|---|
| Bi | Bare bismuth nanoparticles |
| Bi–PEG | Polyethylene glycol modified bismuth nanoparticles |
| $Bi@SiO_2$ | Silica encapsulated bismuth nanoparticles |
| $Bi@SiO_2–NH_2$ | Amine modified silica encapsulated bismuth nanoparticles |
| Calcein AM | Calcein acetoxymethyl ester |
| CdSe/ZnS–COOH | Carboxylic acid modified CdSe/ZnS nanoparticles |
| EthD-1 | Ethidium homodimer-1 |
| $Fe_3O_4$–COOH | Carboxylic acid modified iron oxide nanoparticles |
| $Fe_3O_4–NH_2$ | Amine modified iron oxide nanoparticles |
| G6PD | Glucose-6-phosphate dehydrogenase |
| MAA | Mercaptoacetic acid |
| MTT | 3-(4,5-Dimethylthiazol-2-yl)-2,5-diphenyltetrazolium bromide |
| PEG | Polyethylene glycol |
| XRF | X-ray fluorescence |

## 1 Introduction

Being considered as one of the least toxic heavy metal, bismuth has been widely used in industry, biological and medical

sciences. Bismuth has been used in shotgun pellets as a substitute for lead [1]. Bismuth compounds are most commonly used for treating gastrointestinal disorders [2], eradication of *Helicobacter pylori* in peptic ulcers [3–5], treatment of syphilis and tumors [6], reduction of the renal toxicity of cisplatin [7]. Although several double-blind trials have shown that the blood bismuth concentration of 50 μg/L (~600 nM) is considered to be non-toxic during bismuth compound administration, some side effects such as bismuth-induced encephalopathy are still reported [8]. Meanwhile, 5.0 mg/L (~10 μM) bismuth oxide can induce genotoxicity by promoting the oxidative stress in blood [9]. 200 mM bismuth citrate exposed J774 cells accumulate the metal in their lysosomes and result in lysosomal rupture [10]. In vivo toxicity studies also reveal that 100 μg/L colloidal bismuth subnitrate can induce liver damage [11] and cerebellar involvement [12].

Recently, bismuth nanoparticles have drawn great attention in biological sciences such as bioimaging [13, 14], biosensing [15], biomolecular detection [16, 17], and X-ray radiosensitizing [18]. The increasing biological applications promote serious concerns about the toxicity of bismuth nanoparticles, due to their small size and intimate contact with cellular components such as plasma membrane, organelles, DNA and proteins. Thus the cytotoxicity of any nanoparticle should be extensively and carefully addressed before further biological applications. For instance, the toxicity of gold (Au) and iron oxide ($Fe_3O_4$) nanoparticles are well established and are generally considered non-toxic or less toxic and can be used directly; while cadmium selenide/zinc sulfide (CdSe/ZnS) quantum dots are moderately toxic and have to be surface-modified to reduce the toxicity by minimizing direct contact with cellular components or reducing the release of toxic $Cd^{2+}$ [19].

However, comprehensive cytotoxicity information on bismuth nanoparticles is not available. At the same time, it is well known that toxicity of nanoparticles is quite different from their metal compounds because of the higher chemical reactivity and biological activity [20, 21]. Therefore, we have reasons to doubt whether the bismuth nanoparticles is more toxic than its compounds. Due to the intimate contact with cells or tissues in vivo, the cytotoxicity of nanoparticles are largely determined by the physical property of these nanoparticles, such as atomic number, particle diameter, and surface modifications. Among them, the use of various surface modification techniques to decrease nanotoxicity is the mainstream of nanotoxicity researches [22–24]. Nanoparticles with positively charged surfaces can enter cell membrane and cause cell damage due to strong electrostatic interactions. For in vivo applications, nanoparticles are modified with neutral polymers such as polyethylene glycol (PEG) in order to reduce damage to cells while enhancing circulation time in bloodstream [25]. Meanwhile, silica modified nanoparticles show less toxicity in both in vivo and in vitro experiments [26–28]. But, the overall impact of surface coatings on the cytotoxicity of bismuth nanoparticles is still unknown.

Besides, previous studies have revealed that several mechanisms are responsible for nanoparticle-induced cellular damage [29, 30]. Generation of reactive oxygen species (ROS) is the dominant mechanism of cellular damage for most nanomaterials due to their higher chemical reactivities. Release of metal ions from nanoparticle dissolution is another important mechanism for toxicity of some nanoparticles (e.g. Ag, CdTe, CuO) [31–34]. Inhibiting the DNA repair by displacement of $Zn^{2+}$ from the zinc finger protein of DNA repair enzymes also leads to increased DNA damage [35]. Multiple cytotoxicity assays (such as membrane integrity, enzyme activity, reproduction capability, and DNA damage) are needed to elucidate these mechanisms mainly because these toxicity assays always give inconsistent results due to their unique detection principles. For instance, 3- (4,5-dimethylthiazol-2-yl)-2,5-diphenyltetrazolium bromide) (MTT) tests detect integrity of cell membrane and the activity of enzyme in mitochondria, reflecting the degree of damage on mitochondria function; glucose-6-phosphate dehydrogenase (G6PD) assay detect levels of G6PD leaking from damaged cell membranes; Ethidium homodimer-1 (EthD-1) stain detects cells membrane integrity, and calcein acetoxymethyl ester (Calcein AM) stain detects intracellular esterase activities. Considering the different cytotoxicity mechanisms of nanoparticles that affect cells, it is imperative that the combined use of these toxicity assays could provide comprehensive information on nanoparticle cytotoxicity.

This paper focuses on in vitro cytotoxicities of bismuth nanoparticles by combining three different assays (MTT, G6PD and calcein AM/EthD-1) (Fig. 1). Various surface modifications and different concentration of nanoparticles are used to test the toxicity levels on two kinds of mammalian cells (HeLa cell and MG-63 cell). The results are cross-compared to those derived from CdSe/ZnS quantum dots and iron oxide nanoparticles. Our results show that bismuth nanoparticles are more toxic than previously reported bismuth compounds. HeLa cells are more vulnerable to cytotoxicity of various surface modified bismuth nanoparticles than MG-63 cells; and cytotoxicities of surface modified bismuth nanoparticles are in descending order of amine modified nanoparticles (Bi–$NH_2$), bare bismuth nanoparticles (Bi), silica modified nanoparticles (Bi@$SiO_2$), and PEG modified nanoparticles (Bi–PEG).

## 2 Materials and methods

### 2.1 Chemicals

Vybrant MTT cell proliferation kit, vybrant cytotoxicity assay kit, and live/dead viability/cytotoxicity kit are purchased from

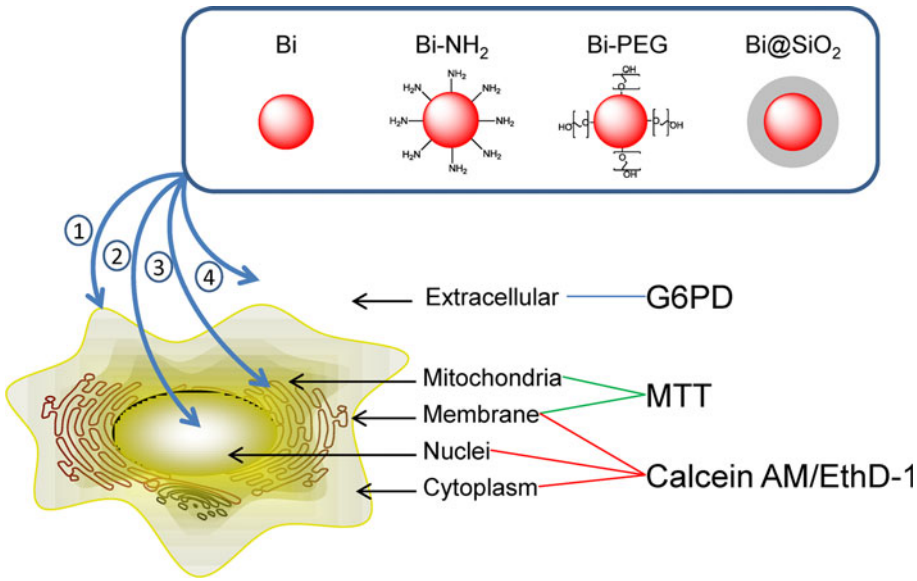


**Fig. 1** Cytotoxicity study of bismuth nanoparticles using multi-end point assays: where nanoparticles combine with membrane (*1*), enter nucleus (*2*), enter cell and affect mitochondrion (*3*), or stay outside of cells (*4*) (Color figure online)

Invitrogen (Carlsbad, CA). Polyethylene glycol-terminated silane (PEG-silane, 472–604 g/mol) is from Gelest (Tullytown, PA). Bi $(CH_3COO)_3$, $BiCl_3$, $NaBH_4$, RPMI 1640 media, penicillin, streptomycin, fetal bovine serum (FBS), and Dulbecco's phosphate-buffered saline (D-PBS) are from Sigma–Aldrich (St. Louis, MO). Anhydrous dimethyl sulfoxide (DMSO), toluene, polyvinylpyrrolidone (PVP), tetraethylorthosilicate (TEOS), 3-aminopropyltriethoxysilane (APTES), iron oleate, octadecence, diphenylether, sodium oleate, and Mercaptoacetic acid (MAA) are from VWR (West Chester, PA). Ultrapure water (18.2 MΩ $cm^{-1}$) from Nanopure System (Barnstead, Kirkland, WA) is used. Synergy HT multimode microplate reader from Biotek (Winooski, VT) is used for absorbance and fluorescence measurements. HeLa (CCL-2) and MG-63 (CRL-1427) cell lines are from American type culture collection (ATCC, Manassas, VA).

## 2.2 Nanoparticles synthesis and characterization

Bismuth nanoparticles are made as follows: 0.1 mmol of $Bi(NO_3)_3$ and 0.5 mmol of PVP are dissolved in 10 ml of *N*,*N*-dimethylformamide (DMF). The mixture is degassed with argon for 15 min under stirring. 0.3 ml of 1 M $NaBH_4$ in water is mixed with 10 ml of DMF and added in the mixture of $Bi(NO_3)_3$ and PVP under vigorous stirring and argon flow for 5 min. The nanoparticles are precipitated by adding acetone, followed by centrifugation, washing with acetone and drying in vacuum.

Iron oxide nanoparticles are prepared by thermally decomposing iron oleate precursors. A solution containing an equimolar mixture of iron oleate (0.2 mol/kg) and a stabilizer, in a high-boiling solvent, is vacuum-dried at 120 °C and heated slowly to reflux for 30 min to allow nanoparticles to grow. The mixtures of octadecence and diphenylether are used as solvents to adjust reflux temperature in the range of 290–375 °C, and to control size of nanoparticles. Sodium oleate and oleic acid are used as stabilizers. After cooling, iron oxide nanoparticles are isolated by applying a standard solvent/nonsolvent procedure with hexane/ethanol pairs.

CdSe nanoparticles are made as described in the Ref. [36]. Briefly, 1 mmol of TOPSe and 1.35 mmol of dimethylcadmium are dissolved in 5 ml of trioctylphospine (TOP), and rapidly injected in a vigorously stirred mixture of 10 g of trioctylphosphine oxide (TOPO) and 5 g of hexadecylamine (HDA) heated to 300 °C. Injection results in an immediate nucleation of nanoparticles, which have a broad adsorption maximum around 450 nm. Further growth occurs at 250–310 °C depending on the desired size. For the synthesis of CdSe/ZnS core–shell nanoparticles, 2.5 ml of crude solution of CdSe nanoparticles is mixed with 5 g of TOPO and 2.5 g of HDA, and heated to 220 °C. The amount of Zn:S stock solution necessary to obtain the desired shell thickness is calculated from the ratio between core and shell volume using bulk lattice parameters of CdSe and ZnS. This amount is then added dropwisely to the vigorously stirred solution of CdSe nanoparticles.

In order to determine the size of synthesized nanoparticles, a suspension of nanoparticles in ethanol is dropped onto carbon coated copper grids and allowed to dry at room temperature. A JEOL 1011 transmission electron microscope (TEM) operated at 100 kV is used to image nanoparticles. Nanoparticles have also been characterized by X-ray diffraction (XRD) analysis, X-ray photoelectron spectrometry (XPS), and dynamic light scattering (DLS). A fluorescence spectrometer is used to measure the fluorescence of CdSe/ZnS core shell nanoparticles. An X-ray spectrometer (Amptek X-123) with Si-PIN photodiode is used to analyze X-ray fluorescence (XRF) emissions of nanoparticles in transmission mode. Both

25 μm thick silver and 250 μm thick aluminum filters are used to reduce background and improve signal-to-noise ratio in low energy (0–15 keV) region of spectrum. XRF spectrum for bare bismuth nanoparticles is obtained at 40 kV and 100 μA after 2 min exposure.

### 2.3 Surface modifications

In order to conjugate with PEG, bismuth nanoparticles are modified by adding 20 μl PEG saline and 1 mg of bismuth nanoparticle into 180 μl of toluene. After reacting under sonication for 3 h at the room temperature, un-reacted PEG saline is removed by centrifugation and wash three times with toluene. In order to make amine ended nanoparticles, bismuth or iron oxide nanoparticles are mixed with 5 % 3-APTES in toluene for 2 h, followed by removal of extra saline by centrifugation and washing with toluene. CdSe/ZnS quantum dots are modified with MAA by mixing 35 μl of MAA with 1 mg of CdSe/ZnS nanoparticles in 500 μl of chloroform under sonication for 2 h, followed by washing with toluene for three times. The un-reacted MAA are removed by dialysis against double deionized water using 3.5 K molecular-weight cutoff (MWCO) membrane for 12 h. The stock solutions of bismuth nanoparticles, silica encapsulated bismuth nanoparticles ($Bi@SiO_2$), $Bi–NH_2$, PEG modified bismuth nanoparticles (Bi–PEG), carboxylic acid modified CdSe/ZnS (CdSe/ZnS–COOH), carboxylic acid modified iron oxide ($Fe_3O_4$–COOH) and amine modified iron oxide ($Fe_3O_4$–$NH_2$) nanoparticles are homogeneously dispersed in sterilized phosphate buffer saline (PBS) at pH = 7.4 prior to use.

### 2.4 Cell culture and nanoparticle treatment

HeLa cell and MG-63 cell purchased from ATCC are used to investigate nanoparticles induced cytotoxicity. All the cells are grown in RPMI 1640 culture media containing penicillin (100 U/ml), streptomycin (100 μg/ml), and 10 % FBS, followed by a culture in a 5 % $CO_2$ incubator at 37 °C according to the protocol from ATCC. The culture medium is removed, and cell layer is rinsed with D-PBS solution to remove all traces of serum. Then 2.0 ml Trypsin–EDTA solution is added to flask to detach cells, and 6.0 ml of medium is added to aspirate cells by gently pipetting. The whole cell concentration is counted with a hemocytometer, and 200 μl of suspension is seeded in each well of 96-well microplate at final concentration of $1 \times 10^5$ cell/ml, followed by culturing in a 5 % $CO_2$ incubator at 37 °C for 2 days. After the cell monolayer becomes 80 % confluence, HeLa cells and MG-63 cells are incubated with Bi, $Bi–NH_2$, Bi–PEG, $Bi@SiO_2$, amine modified $Bi@SiO_2$ ($Bi@SiO_2$–$NH_2$), CdSe/ZnS–COOH, $Fe_3O_4$–COOH and $Fe_3O_4$–$NH_2$ with final concentrations of 0.5, 5.0, and 50 nM, respectively. After 24 h, the media are removed and all wells are washed three times with PBS prior to any toxicity assays.

### 2.5 Cytotoxicity assay

MTT assay is carried out as the following: The medium in each well is removed and replaced with 100 μl of culture medium. 10 μl of 12 mM MTT stock solution is added into each well, as well as into a negative control (100 μl of medium without nanoparticles). After incubation at 37 °C for 4 h, 100 μl of SDS-HCl solution is added to each well and mixed thoroughly using pipette. After incubation at 37 °C for 6 h, each sample is mixed with a pipette, and optical absorbance at 570 nm is recorded. G6PD assay is carried out by following the standard protocol. A 50 μl of 2× resazurin/reaction mixture is added to each well, along with fully lysed cells control and live cell control. All samples are assayed in six duplicates. 1 μl of 100× cell lysis buffer is added to lysed-cell control wells to kill cells. The microplate is incubated at 37 °C for 30 min prior to measuring fluorescence intensity at 580 nm with 530 nm excitation. Calcein AM/EthD-1 assay is carried out as following: 100 μl of D-PBS is added into each well to wash cells in order to dilute serum-containing esterase, which can lead to false positive. A 100 μl of dual fluorescence calcein AM/EthD-1 assay reagents is added into each well and incubated for 30 min at room temperature before fluorescence measurement. A cell-free control is used to measure background fluorescence and these signals were subtracted before later calculations. The percentages of live cells and dead cells are calculated by the equation provide by Invitrogen. A fluorescence microscope from Olympus (BX51M) is used to take fluorescent images.

### 2.6 Statistical evaluation

The data are presented as mean ± standard error (SEM) of six independent experiments, and the error bars in each figure represent the standard error of these six independent experiments. Data are subjected to statistical analysis by one-way analysis of variance (ANOVA) followed by Dunnett's method for multiple comparisons. A value of $P < 0.05$ is considered significant. SPSS 16.0 software is used for the statistical analysis and Origin 8.5 software is used for the graph plotting.

## 3 Results

### 3.1 Characterization and surface modification of synthesized nanoparticles

TEM is used to characterize the morphology of synthesized nanoparticles. Figure 2a shows TEM image of bismuth

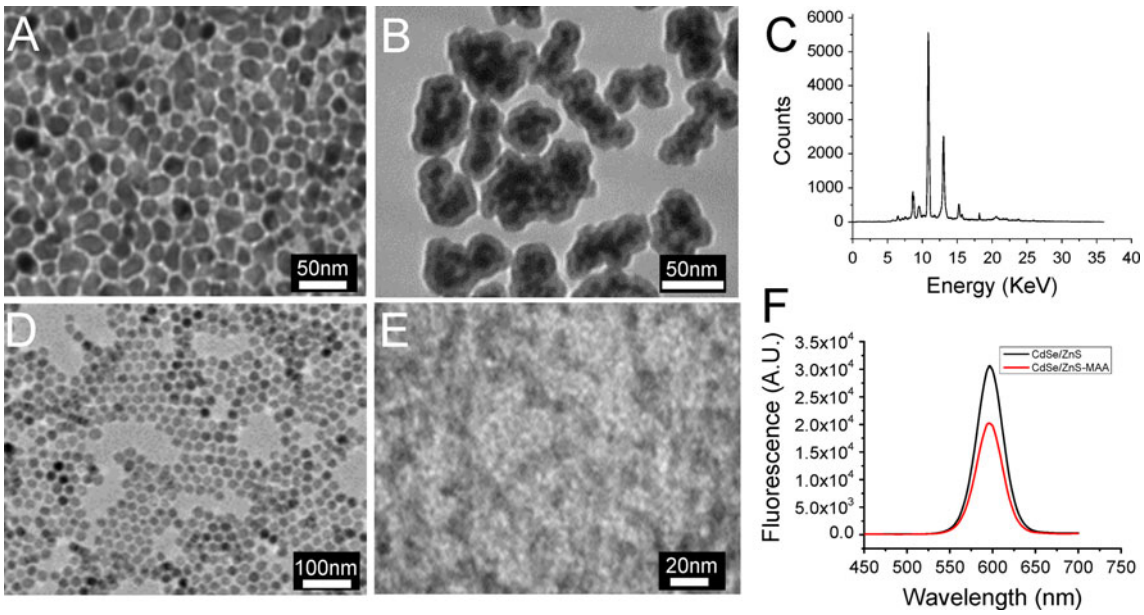


**Fig. 2** TEM image of bismuth nanoparticles (**a**), and silica encapsulated bismuth nanoparticles (**b**); X-ray fluorescence spectrum of bismuth nanoparticles (**c**), TEM image of iron oxide nanoparticles (**d**), and CdSe/ZnS quantum dots (**e**); Fluorescence intensity of CdSe/ZnS quantum dots before (*black*) and after (*red*) conjugation with MAA (**f**) (Color figure online)

nanoparticles, where spherical nanoparticles with diameter of 20 nm, and having rough and porous surfaces, can be seen. Silica coated bismuth nanoparticles have an average thickness of 10 nm and the bismuth core is 20 nm (Fig. 2b). XRF spectrum shows the characteristic $L_{\alpha 1}$ and $L_{\beta 1}$ peaks of bismuth at 10.82 and 13.02 keV, respectively (Fig. 2c). TEM images show that $Fe_3O_4$ nanoparticles (Fig. 2d) and CdSe/ZnS quantum dots (Fig. 2e) have average diameter of 20, and 10 nm, respectively. MAA conjugation chemistry has been adopted in this experiment to transfer CdSe/ZnS quantum dots from organic phase into water phase. The fluorescence intensity decreased about 36 % after the conjugation of MAA on the surface of CdSe/ZnS while the maximum emission wavelength peak remains unchanged (Fig. 2f). The intensity reduction has been addressed by other researches, which could be due to particle loss during washing, or quenching of emission in PBS (pH = 7.4).

### 3.2 Calcein AM/EthD-1 assay

Calcein AM/EthD-1 Dual-fluorescent dying assay can stain the live cells green and the dead cell red simultaneously, providing more comprehensive information of cytotoxicity determination than traditional single-fluorescent assay. Figure 3a–d shows representative fluorescent micrographs of HeLa cells after incubating with 100 ml of 50 mM surface-modified bismuth nanoparticles for 24 h in calcein AM/EthD-1 assay. These figures show that most of the HeLa cells treated by Bi (Fig. 3a) or Bi–$NH_2$ (Fig. 3b) are stained as red (dead), while most of the HeLa cells treated by either Bi@$SiO_2$ (Fig. 3c) or Bi–PEG (Fig. 3d) are stained green (live).

Figure 3e–f shows a nanoparticle concentration-dependent cell viability of both HeLa and MG-63 cells. When the cells are treated by low concentration nanoparticles (0.5 nM), no significant decrease in viability is observed when compared with untreated control ($P < 0.01$). But after exposure to high concentration (50 nM) of nanoparticles, the viabilities of both cells decreased sharply. To eliminate the errors induced by the natural death of cells, a ratio between the nanoparticle-treated cell and untreated control is taken as the viabilities, assuming the viability of untreated control is 100 %, despite the fact that normal cell metabolism processes still produce a small number of dead cells. Figure 3e shows that for HeLa cells, Bi kills 3.2, 15, and 45 % of the cells at nanoparticle concentrations of 0.5, 5.0, 50 nM, respectively; Bi@$SiO_2$ kills 2.3, 17, and 41 % of the cells at these concentrations; Bi–PEG kills 2.5, 13, and 34 % of the cells; and Bi–$NH_2$ kills 2.2, 31, and 52 % of the cells at these nanoparticle concentrations respectively. These data clearly show that all the surface modified bismuth nanoparticles are of low cytotoxicity when the concentration is low (0.5 nM), and the cytotoxicities increase when the nanoparticle concentration increases. Meanwhile, a significant difference in the cytotoxicity is observed when the HeLa cells are exposed to 50 nM bismuth nanoparticles with different modifications. At high nanoparticle concentration (50 nM), Bi–$NH_2$ kills over 50 % of the HeLa cells, while Bi–PEG kills only 34 % HeLa cells, indicating the significant effects of surface

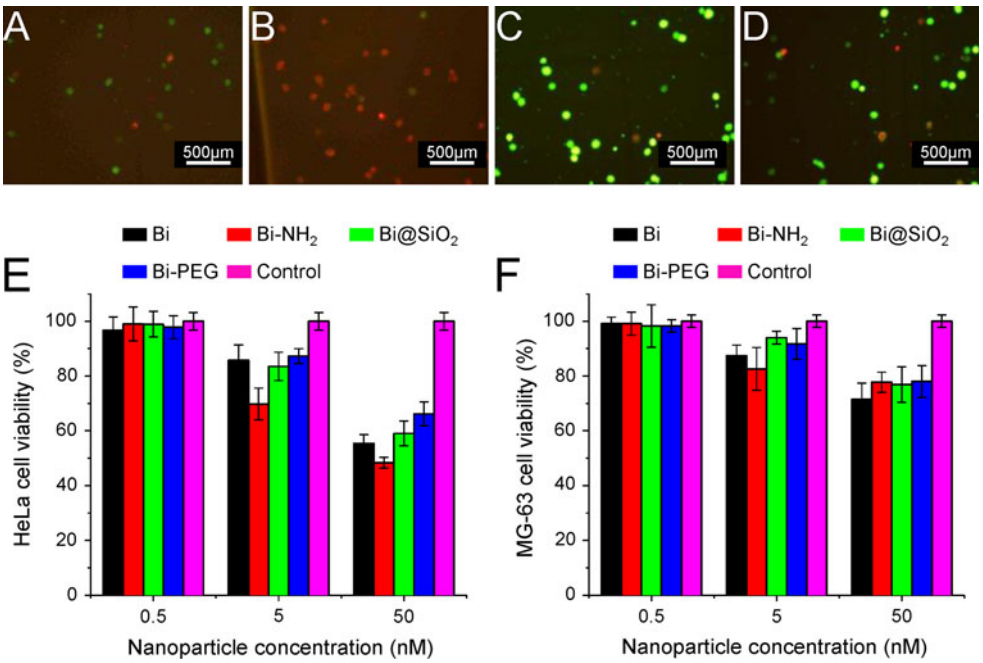


**Fig. 3** Calcein AM/EthD-1 dual-fluorescence stain of HeLa cells that are treated by bismuth nanoparticles (**a**), amine modified bismuth nanoparticles (**b**), silica coated bismuth nanoparticles (**c**), and PEG modified bismuth nanoparticles (**d**); HeLa cell viability after exposing to bismuth nanoparticles (**e**); MG-63 cell viability after exposed to bismuth nanoparticles (**f**) (Color figure online)

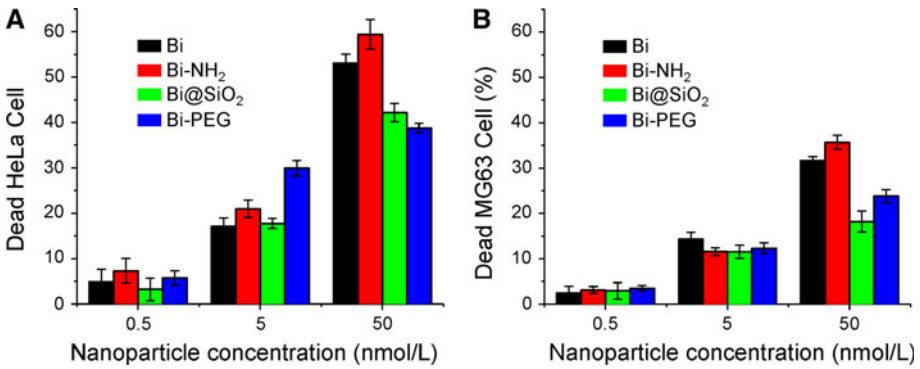


**Fig. 4** G6PD assay of bismuth nanoparticles treated HeLa cells (**a**) and MG-63 cells (**b**), where nanoparticle concentration is 0.5, 5.0, and 50 nM, and incubation time is 24 h (Color figure online)

modifications on the cytotoxicity of bismuth nanoparticles. According to the results above, the toxicities of these nanoparticles on HeLa cells are in the order of Bi–$NH_2$ > Bi > Bi@$SiO_2$ > Bi–PEG.

Figure 3f shows that for MG-63 cells, low concentrations of bismuth nanoparticles kill ~1 % MG-63 cells, showing extremely low cytotoxicities. High concentration (50 nM) of bismuth nanoparticles kill 29, 33, 24, 22 % of MG-63 cells for Bi, Bi–$NH_2$, Bi@$SiO_2$, and Bi–PEG, respectively. Although cytotoxicities of these nanoparticles on MG-63 cells are of the same order as those on HeLa cells (Bi–$NH_2$ > Bi > Bi@$SiO_2$ > Bi–PEG), these bismuth nanoparticles kill less MG-63 cells than HeLa cells when both cells are exposed to the bismuth nanoparticles having the same concentration and the same surface properties. An observation of the higher viability of MG-63 cells than HeLa cells could be 16, 19, 15, 18 % more when they are exposed to 100 ml of 50 nM Bi, Bi–$NH_2$, Bi@$SiO_2$, and Bi–PEG, respectively, indicating that the HeLa cells are more sensitive to the nanotoxicity than MG-63 cells for all the surface modified bismuth nanoparticles.

### 3.3 G6PD assay

G6PD leaking assay is performed to test the membrane integrity by measuring the leaked G6PD levels. Figure 4a, b shows that the viabilities of both HeLa cell and MG-63 cell are concentration-dependent. For HeLa cell (Fig. 4a), low concentration (0.5 nM) of all the surface modified bismuth nanoparticles show low toxicity by killing 5.4, 7.2, 3.5, 6.1 % of the cells for the Bi, Bi–$NH_2$, Bi@$SiO_2$, and Bi–PEG, respectively. And high concentration (50 nM) of bismuth nanoparticles kill 53, 59, 42, 39 % of the cells for Bi, Bi–$NH_2$, Bi@$SiO_2$, and Bi–PEG, respectively. For MG-63 cells (Fig. 4b), these nanoparticles kill 31, 35, 18, 24 % of the cells at 50 nM nanoparticle concentration, which is lower than the number of HeLa cells killed by the same concentration of bismuth nanoparticles.

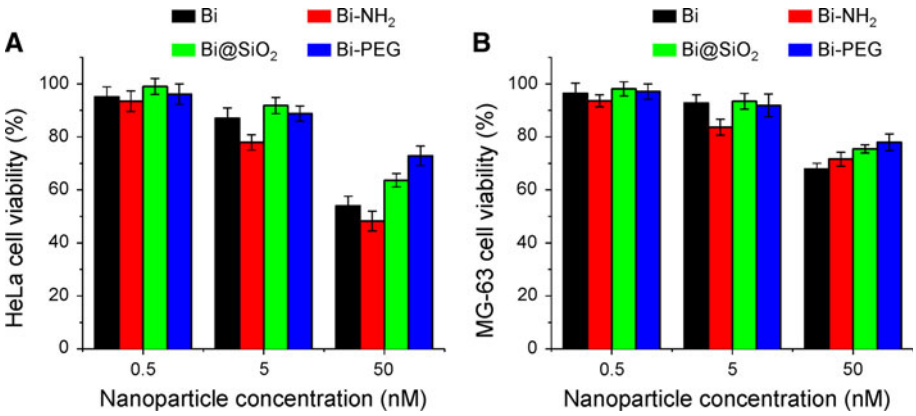


**Fig. 5** MTT assay on bismuth nanoparticles treated HeLa cells (**a**) and MG-63 cells (**b**), where nanoparticle concentration is 0.5, 5.0, and 50 nM, and incubation time is 24 h (Color figure online)

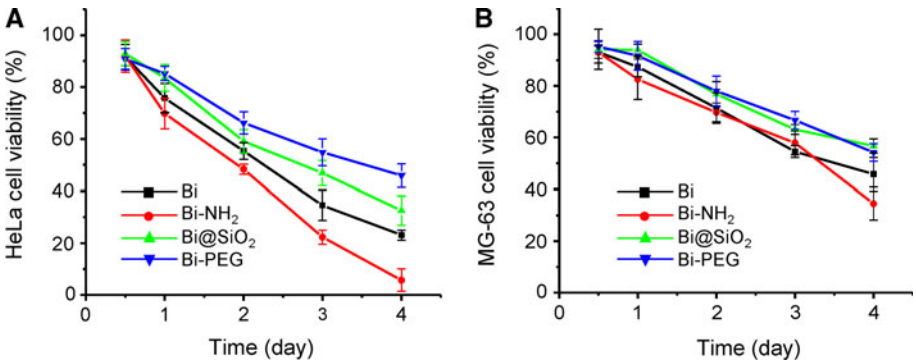


**Fig. 6** Exposure time-dependent cytotoxicity of bismuth nanoparticles on HeLa cells (**a**) and MG-63 cells (**b**), where calcein AM/EthD-1 assay is performed after exposure to nanoparticles for 12, 24, 48, 72, and 96 h (Color figure online)

### 3.4 MTT assay

MTT assay detect the cytotoxicity of nanoparticles by determining the plasma membrane integrity and mitochondrial function, which reflect the metabolism activity. Figure 5a shows that the viabilities of HeLa cells decrease when the bismuth nanoparticle concentrations increase and a dose (or nanoparticle concentration) dependence can be seen as well. For exposure to 50 nM nanoparticles, Bi–$NH_2$ shows the highest nanotoxicity by killing 52 % of the HeLa cells, while Bi@$SiO_2$ and Bi–PEG kill 37 and 28 % of the cells accordingly. This result shows that Bi–$NH_2$ has higher cytotoxicity than bismuth nanoparticles with other surface modifications, and corresponds to the results obtained from calcein AM/EthD-1 analysis. Figure 5b shows that the viability of MG-63 cells treated with Bi–$NH_2$ is much lower than those treated with bismuth nanoparticles with other surface properties. PEG-modified bismuth nanoparticles have shown lowest toxicity for both HeLa cells and MG-63 cells, because PEG has extremely low sticking energy to cells.

### 3.5 Cell viability after different treating time

The increased nanoparticle exposure time can decrease the viability of nanoparticle-treated mammalian cells. Since results from calcein AM/EthD-1, MTT, and G6PD assays are very consistent, calcein AM/EthD-1 assay is taken to derive viability of cells after different nanoparticle exposure time. Figure 6a shows the HeLa viability after treated with 100 ml of 50 nM surface modified bismuth nanoparticles for different times. There are ~7 % HeLa cells killed after exposure for 12 h; there is no difference between these four surface modified bismuth nanoparticles. After 24 h, the HeLa cell viabilities are 24, 31, 17, 15 % for Bi, Bi–$NH_2$, Bi@$SiO_2$, and Bi–PEG, respectively. After 4 days (94 h), the viability decreases to 23, 5.7, 32, 46 %, respectively. Cells viability decreases when exposure time continuously increases. Figure 6b shows the similar time-dependent relations. But the 4-day exposure only kills 54, 65, 43, 46 % of the MG-63 cells for Bi, Bi–$NH_2$, Bi@$SiO_2$, and Bi–PEG treatment, which is much lower than those from HeLa cells. These results show that the HeLa cells are more sensitive to bismuth nanoparticles than MG-63 cells, which is identical to the cytotoxicity of bismuth nanoparticles derived from MTT and G6PD assays.

### 3.6 Comparison of toxicity between bismuth, CdSe/ZnS, and $Fe_3O_4$ nanoparticles

The nanotoxicity of bismuth nanoparticles on HeLa cell and MG-63 cell are compared to those of CdSe/ZnS and $Fe_3O_4$. Bi@$SiO_2$ is reacted with APTES to make Bi@$SiO_2$–$NH_2$. For 100 ml of 50 nM nanoparticles

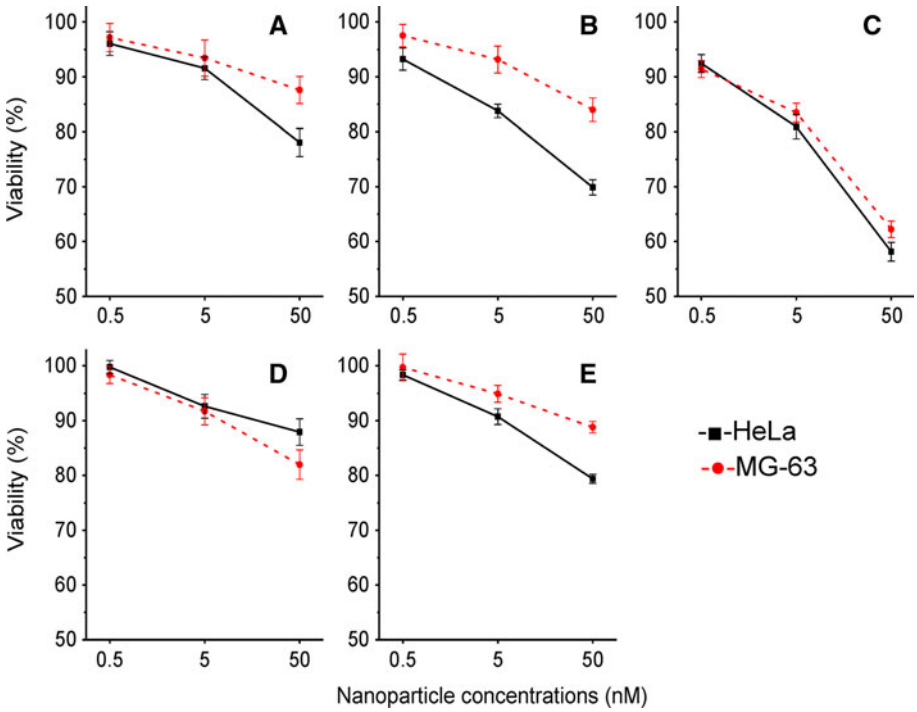


**Fig. 7** Cytotoxicity of $Bi@SiO_2$ (**a**), $Bi@SiO_2$–$NH_2$ (**b**), CdSe/ZnS–COOH nanoparticles (**c**), $Fe_3O_4$–COOH (**d**), and $Fe_3O_4$–$NH_2$ (**e**) on HeLa cell and MG-63 cell at nanoparticle concentration of 0.5, 5.0 and 50 nM, where calcein AM/EthD-1 assay is used to test cytotoxicity. (*black square*) is from HeLa cell, and (*black circle*) is from MG-63 cell (Color figure online)

exposure, calcein AM results shows that $Bi@SiO_2$ (Fig. 7a) and $Bi@SiO_2$–$NH_2$ (Fig. 7b) kill 14 and 52 % HeLa cells, respectively, while CdSe/ZnS-$NH_2$ demonstrate a much higher toxicity by killing 48 % HeLa cells (Fig. 7c). $Fe_3O_4$–COOH (Fig. 7d) or $Fe_3O_4$–$NH_2$ (Fig. 7e) shows a relatively low cytotoxicity by killing 13 and 22 % cells, respectively. For nanoparticles of different core, the cytotoxicity are in the order of CdSe/ZnS > $Bi@SiO_2$ > $Fe_3O_4$ and the toxicity of $Bi@SiO_2$ varied significantly according to the surface modifications. The high cytotoxicities of CdSe/ZnS-$NH_2$ have been reported by others, which are mainly attributed to the release of toxic $Cd^{2+}$. For different surface modification of the same nanoparticles, $Fe_3O_4$–$NH_2$ is more toxic than $Fe_3O_4$–COOH to HeLa cells by killing 9 % more HeLa cells. Similarly, $Bi@SiO_2$–$NH_2$ is more toxic than $Bi@SiO_2$. Thus, amine group modification can increase cytotoxicity of nanoparticles more than other surface modifications.

A dose-dependent cytotoxicity is also observed for MG-63 cell. As expected, the CdSe/ZnS nanoparticles give strongest cytotoxicity when compared with iron oxide and bismuth nanoparticles. 50 nM $Fe_3O_4$–COOH kills 5 % more MG-63 cells than 50 nM $Fe_3O_4$–$NH_2$ does, indicating $Fe_3O_4$–$NH_2$ is less toxic than $Fe_3O_4$–COOH. This result is opposite to the toxicity derived from the HeLa cells, which could be explained by cell-type-dependent cytotoxicity of nanoparticles [37]. The adhesion of nanoparticles on cell surface is prerequisites for nanoparticles entering cells via endocytosis. Different proteins or cytokines are excreted on surface of HeLa cells or MG-63 cell. Proteins on HeLa cells tend to adhere to carboxyl group, while those on MG-63 cells tend to adhere to amine group. This adherence of nanoparticles on cell surface mediates the penetration of nanoparticles, thus accelerating cell death by releasing ROS.

## 4 Discussions

Despites their potentials in bioimaging and radiosensitizing, there is no cytotoxicity study on bismuth nanoparticles. Experiments on bismuth nanoparticles still rely on available cytotoxicity data on bismuth compound, which is the least toxic among the heavy metals. But, the toxicity of bismuth nanoparticles maybe different from that of bismuth compound due to their large surface area and surface property. Indeed, toxicity of nanoparticles is quite different from those of metal compounds or salts. Silver and copper nanoparticles have been reported to be more toxic than silver ions [33, 38], and copper salts [39], respectively. Unlike metal compounds, metal nanoparticles are easy to be modified, and surface modified nanoparticles may have different cytotoxicity. The most frequently used surface modification is PEGylation of metal nanoparticles to decrease cell adhesion, thus reduce cytotoxicity and enhance circulation [25, 40]. This study is focused on two issues related to bismuth nanoparticles: (1) what is the cytotoxicity of bismuth nanoparticles, and (2) what is the effect of surface modifications on cytotoxicity of bismuth nanoparticles?

Three types of nanoparticles ($Bi@SiO_2$, CdSe/ZnS, $Fe_3O_4$) have been made, where CdSe/ZnS and $Fe_3O_4$ nanoparticles are used as the controls. Our results show that CdSe/ZnS is the most toxic one among three types of

nanoparticles by killing ~15 % more HeLa cells than $Bi@SiO_2$ and 20 % more than $Fe_3O_4$ nanoparticles. This is in accordance with previous reports that CdSe/ZnS nanoparticle is more toxic than $Fe_3O_4$ nanoparticle at the same surface modification [19, 32, 41–43]. The higher toxicity of CdSe/ZnS is mainly due to releasing of cadmium ion ($Cd^{2+}$) and formation of ROS after being digested into the cytoplasm [37]. The lower toxicity of $Fe_3O_4$ is perhaps because the released iron ions ($Fe^{3+}$) are transferred and utilized by red blood cells. The toxicity of bismuth is relatively low, mainly because released bismuth ions ($Bi^{3+}$) are the least toxic among all heavy metals.

Bismuth nanoparticles have been modified to have surrounding $NH_2$, COOH, silica, and PEG. Silica encapsulated bismuth nanoparticles cannot be treated as silica nanoparticles, because culture medium diffuses into porous silica shell, and takes out bismuth ions. $Bi@SiO_2$ and Bi–PEG can reduce 20 and 24 % of toxicity of the Bi. Bi–PEG has the lowest toxicity due to low zeta potential and reduced interaction with receptors. Because most receptors, that mediate specific interactions between cells and their extracellular milieu, are located on plasma membrane [44], the non-adhesive Bi–PEG cannot be internalized through mediation of receptors, and has low cytotoxicity [45]. The cytotoxicity of insulin-immobilized CdS nanoparticles was greatly suppressed by using PEG as spacer [25]. PEG grafting can also reduce toxicity of gold nanoparticles, where chain length does not affect cell internalization [46]. On the other hand, $Bi@SiO_2$ is less toxic than bismuth nanoparticles, because silica shell is a barrier between cell and nanoparticle and retards mobilization of bismuth ion into cell, thereby reducing oxidative stress. This explanation is also supported by an experiment on cytotoxicity of silica modified magnetic nanoparticles [47]. Though $Bi@SiO_2$ is less toxic than bismuth nanoparticle, the thickness of silica shell does not have significant effect on cell viability, probably because 20 nm silica shell is thick enough to retard mobilization of bismuth ions.

We further compared the toxicity of bismuth nanoparticles with the bismuth compounds reported by other studies. Several double-blind trails show those have bismuth blood level values below 50 μg/l (~600 nM) are highly unlikely to be associated with meaningful toxicity in man [48]. Von Recklinghausen et al. [35] report that 4 μM methylbismuth compound is toxic, while bismuth citrate and bismuth glutathione are not genotoxic on human lymphocytes and hepatocytes even at high concentration of 500 μM. Tomohiro et al. compared the toxicity of triphenylbismuth and bismuth chloride [49]. They found that the 10–30 μM bismuth chloride did not significantly affect cell viability and the threshold of triphenylbismuth affecting thymocytes viability was 3 μM. Similarly, Ribeiro et al. [50] found 100 μg/ml bismuth oxide (equals to 215 nM) is not genotoxic by the single-cell gel assay. On the contrary, bismuth nanoparticles at concentration of 50 nM may have considerable cytotoxicity by killing ~45 % HeLa cells. The concentrations (0.5, 5.0, 50 nM) in our experiments are much lower than the previous reports (at least 215 nM), thus we think the bismuth nanoparticles are more toxic than the bismuth compounds at the same molar concentration. The increased toxicity of bismuth nanoparticles over bismuth compounds may be caused by size effect and release of bismuth ion. Similar results have been found in other nanoparticles. Silver nanoparticles have been reported to be more toxic than $Ag^+$ [38], and the increased toxicity of silver nanoparticles is mainly explained as nanoparticles induced killing, and toxicity of released $Ag^+$. Similarly, copper nanoparticles show higher toxicity on zebrafish than soluble copper salts, which is also due to the higher toxicity of released copper ions ($Cu^{2+}$) [39].

Three assays (MTT, G6PD, and calcein AM/EthD-1) are used in combination to provide complementary information on cytotoxicity of bismuth nanoparticles. MTT tests detect integrity of cell membrane and activity of enzyme in mitochondria, which reflects function of mitochondria. G6PD assay detects G6PD leaking when cell membrane is damaged. EthD-1 detects integrity of membrane; while calcein AM detects activity of intracellular esterase. The difference between G6PD leaking and MTT can be explained by the fact that cell metabolic activity is less affected even though plasma membrane is damaged. If this phenomenon exists in differently modified nanoparticles, it means that surface modified nanoparticles can damage the cells, yet cannot damage mitochondria of cells. Therefore, the mechanism of nanoparticle-cell interaction can be revealed at least partially by combining multiple in vitro assays that have different end-points. Bi–PEG treated cells have shown different viability in MTT assay (28 %) and G6PD assay (39 %), suggesting that Bi–PEG affects less on cell mitochondria. Because Bi–PEG does not have strong affinity to proteins secreted on cell surface, most of Bi–PEG nanoparticles are expelled outside cell membrane. $Bi@SiO_2$ can enter cell membrane, and have effect on activity of intracellular esterase, while it has less effect on mitochondria, indicating the toxicity of $Bi@SiO_2$ is less related to metabolic function. $Bi–NH_2$ shows similar viability in MTT and G6PD assay, suggesting that damage to mitochondria function is consistent with damage to plasma membrane, and cytotoxicity of $Bi–NH_2$ is mainly due to compromised metabolic function.

The mechanisms of nanoparticle induced damage to the cells are complicated, involving the release of metal ions, production of ROS, and combination with zinc finger proteins. Hence, it is very difficult to elucidate the damage of human cells with one of these hypotheses. Thus, further research is needed to explore the actual mechanisms of bismuth nanoparticle induced damage to human cells.

## 5 Conclusion

The cytotoxicity of bismuth nanoparticles is studied on HeLa cells and MG-63 cells by combining three assays (MTT, G6PD, and calcein AM/EthD-1). The toxicity of bismuth nanoparticles is higher than those reported for bismuth chloride at the same molar concentration. HeLa cell is more susceptible to cytotoxicity of bismuth nanoparticles than MG-63 cell. Bismuth nanoparticles are less toxic than CdSe/ZnS at the same nanoparticle concentration and has similar toxicity as iron oxide nanoparticles. Surface modifications have significant impact on cytotoxicity of bismuth nanoparticles. The cell viability (MTT, G6PD, and calcein AM/EthD-1) are in sequence of Bi–$NH_2$, Bi, Bi@$SiO_2$, and Bi–PEG (from lowest to highest). The combined use of complementary toxicity assays can provide more information on cytotoxicity of nanoparticles.

**Acknowledgments** This project has been supported by a research grant (0828466), a CAREER award from National Science Foundation, a Concept Award (W81XWH-10-1-0961) from Lung Cancer Research Program of Department of Defense, a grant from the National Natural Science Foundation of China (30900348), and a fund for the transformation of scientific and technological achievements of the Third Military Medical University (2010XZH08).

## References

1. Pamphlett R, Danscher G, Rungby J, Stoltenberg M. Tissue uptake of bismuth from shotgun pellets. Environ Res. 2000;82:258–62.
2. Larsen A, Martiny M, Stoltenberg M, Danscher G, Rungby J. Gastrointestinal and systemic uptake of bismuth in mice after oral exposure. Pharmacol Toxicol. 2003;93:82–90.
3. Andrews PC, Ferrero RL, Forsyth CM, Junk PC, Maclellan JG, Peiris RM. Bismuth(III) saccharinate and thiosaccharinate complexes and the effect of ligand substitution on their activity against *Helicobacter pylori*. Organometallics. 2011;30:6283–91.
4. Gisbert JP. *Helicobacter pylori* eradication: a new, single-capsule bismuth-containing quadruple therapy. Nat Rev Gastroenterol Hepatol. 2011;8:307–9.
5. Malfertheiner P, Bazzoli F, Delchier JC, Celinski K, Giguere M, Riviere M, et al. *Helicobacter pylori* eradication with a capsule containing bismuth subcitrate potassium, metronidazole, and tetracycline given with omeprazole versus clarithromycin-based triple therapy: a randomised, open-label, non-inferiority, phase 3 trial. Lancet. 2011;377:905–13.
6. Rosenblat TL, McDevitt MR, Mulford DA, Pandit-Taskar N, Divgi CR, Panageas KS, et al. Sequential cytarabine and alpha-particle immunotherapy with bismuth-213-lintuzumab (HuM195) for acute myeloid leukemia. Clin Cancer Res. 2010;16:5303–11.
7. Leussink BT, Baelde HJ, Broekhuizen-van den Berg TM, de Heer E, van der Voet GB, Slikkerveer A, et al. Renal epithelial gene expression profile and bismuth-induced resistance against cisplatin nephrotoxicity. Hum Exp Toxicol. 2003;22:535–40.
8. Larsen A, Stoltenberg M, West MJ, Danscher G. Influence of bismuth on the number of neurons in cerebellum and hippocampus of normal and hypoxia-exposed mouse brain: a stereological study. J Appl Toxicol. 2005;25:383–92.
9. Geyikoglu F, Turkez H. Genotoxicity and oxidative stress induced by some bismuth compounds in human blood cells in vitro. Fresenius Environ Bull. 2005;14:854–60.
10. Stoltenberg M, Larsen A, Zhao M, Danscher G, Brunk UT. Bismuth-induced lysosomal rupture in J774 cells. APMIS. 2002;110:396–402.
11. Turkez H, Geyikoglu F, Keles MS. Biochemical response to colloidal bismuth subcitrate—dose–time effect. Biol Trace Elem Res. 2005;105:151–8.
12. Stoltenberg M, Hogenhuis JA, Hauw JJ, Danscher G. Autometallographic tracing of bismuth in human brain autopsies. J Neuropathol Exp Neurol. 2001;60:705–10.
13. Kinsella JM, Jimenez RE, Karmali PP, Rush AM, Kotamraju VR, Gianneschi NC, et al. X-ray computed tomography imaging of breast cancer by using targeted peptide-labeled bismuth sulfide nanoparticles. Angew Chem Int Ed. 2011;50:12308–11.
14. Rabin O, Manuel Perez J, Grimm J, Wojtkiewicz G, Weissleder R. An X-ray computed tomography imaging agent based on long-circulating bismuth sulphide nanoparticles. Nat Mater. 2006;5:118–22.
15. Ding SN, Shan D, Xue HG, Cosnier S. A promising biosensing-platform based on bismuth oxide polycrystalline-modified electrode: characterization and its application in development of amperometric glucose sensor. Bioelectrochemistry. 2010;79:218–22.
16. Ma L, Hong Y, Ma Z, Kaittanis C, Perez JM, Su M. Multiplexed highly sensitive detections of cancer biomarkers in thermal space using encapsulated phase change nanoparticles. Appl Phys Lett. 2009;95:043701.
17. Wang C, Sun Z, Ma L, Su M. Simultaneous detection of multiple biomarkers with over three orders of concentration difference using phase change nanoparticles. Anal Chem. 2011;83:2215–9.
18. Hossain M, Wang C, Su M. Multiplexed biomarker detection using X-ray fluorescence of composition-encoded nanoparticles. Appl Phys Lett. 2010;97:263704.
19. Wang L, Nagesha DK, Selvarasah S, Dokmeci MR, Carrier RL. Toxicity of CdSe nanoparticles in Caco-2 cell cultures. J Nanobiotechnol. 2008;6:11.
20. Zhao J, Castranova V. Toxicology of nanomaterials used in nanomedicine. J Toxicol Environ Health B Crit Rev. 2011;14:593–632.
21. Zhang Y, Yu W, Jiang X, Lv K, Sun S, Zhang F. Analysis of the cytotoxicity of differentially sized titanium dioxide nanoparticles in murine MC3T3-E1 preosteoblasts. J Mater Sci Mater Med. 2011;22:1933–45.
22. Clift MJ, Rothen-Rutishauser B, Brown DM, Duffin R, Donaldson K, Proudfoot L, et al. The impact of different nanoparticle surface chemistry and size on uptake and toxicity in a murine macrophage cell line. Toxicol Appl Pharmacol. 2008;232:418–27.
23. Zhu ZJ, Carboni R, Quercio MJ Jr, Yan B, Miranda OR, Anderton DL, et al. Surface properties dictate uptake, distribution, excretion, and toxicity of nanoparticles in fish. Small. 2010;6:2261–5.
24. Hoshino A, Hanada S, Yamamoto K. Toxicity of nanocrystal quantum dots: the relevance of surface modifications. Arch Toxicol. 2011;85:707–20.
25. Selim KK, Xing ZC, Choi MJ, Chang Y, Guo H, Kang IK. Reduced cytotoxicity of insulin-immobilized CdS quantum dots using PEG as a spacer. Nanoscale Res Lett. 2011;6:528.
26. Zhang XD, Wu D, Shen X, Liu PX, Yang N, Zhao B, et al. Size-dependent in vivo toxicity of PEG-coated gold nanoparticles. Int J Nanomed. 2011;6:2071–81.
27. Cho WS, Cho MJ, Jeong J, Choi M, Cho HY, Han BS, et al. Acute toxicity and pharmacokinetics of 13 nm-sized PEG-coated gold nanoparticles. Toxicol Appl Pharmacol. 2009;236:16–24.

28. Malugin A, Ghandehari H. Cellular uptake and toxicity of gold nanoparticles in prostate cancer cells: a comparative study of rods and spheres. J Appl Toxicol. 2010;30:212–7.
29. Nair S, Sasidharan A, Divya Rani VV, Menon D, Manzoor K, Raina S. Role of size scale of ZnO nanoparticles and microparticles on toxicity toward bacteria and osteoblast cancer cells. J Mater Sci Mater Med. 2009;20(Suppl 1):S235–41.
30. Wang H, Wingett D, Engelhard MH, Feris K, Reddy KM, Turner P, et al. Fluorescent dye encapsulated ZnO particles with cell-specific toxicity for potential use in biomedical applications. J Mater Sci Mater Med. 2009;20:11–22.
31. Zhao Y, Lin K, Zhang W, Liu L. Quantum dots enhance $Cu^{2+}$-induced hepatic L02 cells toxicity. J Environ Sci (China). 2010;22:1987–92.
32. Mahmoudi M, Simchi A, Imani M, Milani AS, Stroeve P. An in vitro study of bare and poly(ethylene glycol)-co-fumarate-coated superparamagnetic iron oxide nanoparticles: a new toxicity identification procedure. Nanotechnology. 2009;20:225104.
33. Johnston HJ, Hutchison G, Christensen FM, Peters S, Hankin S, Stone V. A review of the in vivo and in vitro toxicity of silver and gold particulates: particle attributes and biological mechanisms responsible for the observed toxicity. Crit Rev Toxicol. 2010;40:328–46.
34. Yan M, Zhang Y, Xu K, Fu T, Qin H, Zheng X. An in vitro study of vascular endothelial toxicity of CdTe quantum dots. Toxicology. 2011;282:94–103.
35. von Recklinghausen U, Hartmann LM, Rabieh S, Hippler J, Hirner AV, Rettenmeier AW, et al. Methylated bismuth, but not bismuth citrate or bismuth glutathione, induces cyto- and genotoxic effects in human cells in vitro. Chem Res Toxicol. 2008;21:1219–28.
36. Talapin DV, Rogach AL, Kornowski A, Haase M, Weller H. Highly luminescent monodisperse CdSe and CdSe/ZnS nanocrystals synthesized in a hexadecylamine–trioctylphosphine oxide–trioctylphospine mixture. Nano Lett. 2001;1:207–11.
37. Kirchner C, Liedl T, Kudera S, Pellegrino T, Munoz Javier A, Gaub HE, et al. Cytotoxicity of colloidal CdSe and CdSe/ZnS nanoparticles. Nano Lett. 2005;5:331–8.
38. Navarro E, Piccapietra F, Wagner B, Marconi F, Kaegi R, Odzak N, et al. Toxicity of silver nanoparticles to *chlamydomonas reinhardtii*. Environ Sci Technol. 2008;42:8959–64.
39. Griffitt RJ, Weil R, Hyndman KA, Denslow ND, Powers K, Taylor D, et al. Exposure to copper nanoparticles causes gill injury and acute lethality in zebrafish (Danio rerio). Environ Sci Technol. 2007;41:8178–86.
40. Pittella F, Zhang M, Lee Y, Kim HJ, Tockary T, Osada K, et al. Enhanced endosomal escape of siRNA-incorporating hybrid nanoparticles from calcium phosphate and PEG-block charge-conversional polymer for efficient gene knockdown with negligible cytotoxicity. Biomaterials. 2011;32:3106–14.
41. Tiwari DK, Jin T, Behari J. Bio-distribution and toxicity assessment of intravenously injected anti-HER2 antibody conjugated CdSe/ZnS quantum dots in Wistar rats. Int J Nanomed. 2011;6:463–75.
42. Naqvi S, Samim M, Abdin M, Ahmed FJ, Maitra A, Prashant C, et al. Concentration-dependent toxicity of iron oxide nanoparticles mediated by increased oxidative stress. Int J Nanomed. 2010;5:983–9.
43. Mahmoudi M, Simchi A, Milani AS, Stroeve P. Cell toxicity of superparamagnetic iron oxide nanoparticles. J Colloid Interface Sci. 2009;336:510–8.
44. Gupta AK, Berry C, Gupta M, Curtis A. Receptor-mediated targeting of magnetic nanoparticles using insulin as a surface ligand to prevent endocytosis. IEEE Trans Nanobiosci. 2003;2:255–61.
45. Park J, Fong PM, Lu J, Russell KS, Booth CJ, Saltzman WM, et al. PEGylated PLGA nanoparticles for the improved delivery of doxorubicin. Nanomedicine. 2009;5:410–8.
46. Liu Y, Shipton MK, Ryan J, Kaufman ED, Franzen S, Feldheim DL. Synthesis, stability, and cellular internalization of gold nanoparticles containing mixed peptide-poly(ethylene glycol) monolayers. Anal Chem. 2007;79:2221–9.
47. Baber O, Jang M, Barber D, Powers K. Amorphous silica coatings on magnetic nanoparticles enhance stability and reduce toxicity to in vitro BEAS-2B cells. Inhal Toxicol. 2011;23:532–43.
48. Serfontein WJ, Mekel R. Bismuth toxicity in man II. Review of bismuth blood and urine levels in patients after administration of therapeutic bismuth formulations in relation to the problem of bismuth toxicity in man. Res Commun Chem Pathol Pharmacol. 1979;26:391–411.
49. Arata T, Oyama Y, Tabaru K, Satoh M, Hayashi H, Ishida S, et al. Cytotoxic effects of triphenylbismuth on rat thymocytes: comparisons with bismuth chloride and triphenyltin chloride. Environ Toxicol. 2002;17:472–7.
50. Ribeiro DA, Carlin V, Fracalossi ACC, Oyama LM. Radiopacifiers do not induce genetic damage in murine fibroblasts: an in vitro study. Int Endod J. 2009;42:987–91.